Mutual Coupling Between Rectangular Slot Antennas on a Conducting Concave Spherical Surface

KAZUYOSHI INAMI, KUNIO SAWAYA, MEMBER, IEEE, AND YASUTO MUSHIAKE, FELLOW, IEEE

Abstract—**The surface fields excited by a horizontal magnetic source located on a conducting concave spherical surface have been formulated. The field expressions are obtained as a combination of ray-optical fields and simplified integrals under the condition that the radius of the spherical surface is much greater than the wavelength. Numerical calculations have been performed, and the calculated results for the surface fields have been corroborated with experiments. The results of these basic studies have been used in calculating the mutual coupling between rectangular slot antennas on the conducting concave spherical surface assuming the aperture field as the dominant mode in the wave guides connected with the slots. The numerical results have been compared with those for slots on a convex conducting surface. Experimental investigation of the mutual coupling has also been carried out.**

I. INTRODUCTION

RECENT developments of dome antennas [1], [2] composed of hemispherical or cylindrical lenses and planar array antennas for extending the scanning area have stimulated interests in estimating the mutual coupling between radiating elements on the conducting concave surface as well as on the convex surface.

It is well-known that the conventional geometrical optics is not applicable in the analysis of the surface fields excited by sources on a concave surface [3], [4]. Under this circumstance, some papers have been published describing the surface fields excited by sources located on a cylindrical concave surface [3]–[7]. Babich and Buldyrev [5] have expressed the field of a line source, which has asymptotic properties reaching the observation point along a direct propagation path. They have also derived the high-frequency approximation of the field expressions given by a combination of ray-optical fields and simplified integrals. Based on these field expressions, alternative high-frequency field representations have been discussed by Ishihara *et al.* [4]. These analyses have been extended to the cases of a line source located on a concave cylindrical impedance surface [6] and a point source located on a perfectly conducting concave cylindrical surface [7].

However, these analyses are restricted to the case of cylindrical surface, and problems related to a spherical concave surface are still to be studied. These are important particularly in connection with a spherical dome antenna. Recently, the authors [8] have presented the results of theoretical and experimental studies of the surface fields excited by a vertical electric point source located on a conducting concave spherical surface. The analysis in the paper [8] is based on the method of Babich and Buldyrev [5], and the field expressions have been obtained as a combination of ray-optical fields and simplified integrals. The validity of the analysis has been confirmed by experimental data.

In this paper, mutual coupling between rectangular slot antennas located on the concave side of a spherical surface is presented. First, the expressions of the surface fields excited by a horizontal magnetic point source have been formulated by a procedure similar to that in the previous paper [8]. Subsequently, the mutual coupling has been calculated and compared with that for slots on the convex side reported by Nakashima *et al.* [9].

II. FIELD EXPRESSIONS

The geometry of the problem is illustrated in Fig. 1, where a is the radius of the conducting spherical surface. The magnetic point source $\mathbf{M}$ is located on the concave surface at the z-axis and directed parallel to the x-axis:

$$\mathbf{M} = M_0 \frac{\delta(r-a)\delta(\theta)}{2\pi r^2 \sin\theta} \mathbf{e}_x, \tag{1}$$

where $\delta(\cdot)$ denotes the Dirac delta function. The magnetic fields excited by the source inside the closed sphere are expressed as follows:

$$\left.\begin{matrix} H_\theta \\ H_\phi \end{matrix}\right\} = \mp \frac{M_0}{4\pi\zeta_0 a r} \begin{cases} \cos\phi \left[\dfrac{1}{\sin\theta} u^c(r,\theta) - \dfrac{\partial}{\partial\theta} v^c(r,\theta) \right], & (2a) \\ \sin\phi \left[\dfrac{\partial}{\partial\theta} u^c(r,\theta) - \dfrac{1}{\sin\theta} v^c(r,\theta) \right], & (2b) \end{cases}$$

where $\zeta_0 = \sqrt{\mu_0/\epsilon_0}$ is the intrinsic impedance of free space. The superscript c refers to the closed sphere. The functions u^c and v^c appearing in (2) are given by

$$\left.\begin{matrix} u^c \\ v^c \end{matrix}\right\} = j \sum_{n=1}^{\infty} (2n+1) P_n^{-1}(\cos\theta) \begin{cases} j_n(kr)/j_n'(ka), & (3a) \\ j_n'(kr)/j_n(ka), & (3b) \end{cases}$$

where P_n^{-1} is the associated Legendre function of order $(n, -1)$ and k is the free space wavenumber. The spherical Bessel functions j_n and $h_n^{(1,2)}$ [10] are defined by

$$\left.\begin{aligned} j_n(\eta) &= \sqrt{\pi\eta/2}\, J_{n+1/2}(\eta), \\ h_n^{(1,2)}(\eta) &= \sqrt{\pi\eta/2}\, H_{n+1/2}^{(1,2)}(\eta), \end{aligned}\right\} \tag{4}$$

Manuscript received May 21, 1981; revised December 28, 1981. This work was supported in part by the Mitsubishi Electric Corporation.

K. Inami is with Communication Equipment Works, Mitsubishi Electric Corporation, Amagasaki, 661 Japan.

K. Sawaya and Y. Mushiake are with Department of Electrical Communications, Tohoku University, Aramaki Aoba, Sendai, 980 Japan.

0018-926X/82/0900-0927$00.75

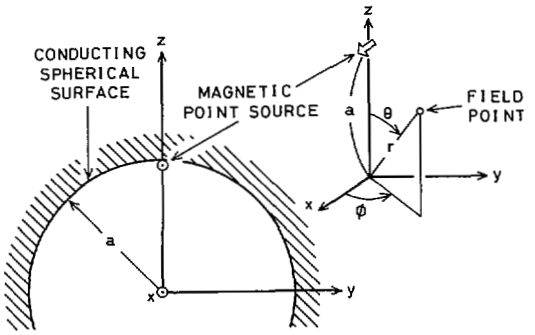

Fig. 1. Geometry of problem. Horizontal magnetic dipole source is located on conducting concave spherical surface.

and the prime on these functions denotes the derivative with respect to the argument.

Starting from (3) and introducing the Watson transformation [10], u^c and v^c can be expressed as follows:

$$u^c = U^c + U_0{}^c, \qquad v^c = V^c + V_0{}^c, \tag{5}$$

$$\left.\begin{matrix} U^c \\ V^c \end{matrix}\right\} = \int_{c_\nu} \frac{\nu P_p{}^{-1}(-\cos\theta)}{\cos\nu\pi} \cdot \begin{cases} j_p(kr)/j_p'(ka)\, d\nu, & (6a) \\ j_p'(kr)/j_p(ka)\, d\nu, & (6b) \end{cases}$$

$$p = \nu - 1/2, \tag{6c}$$

$$\left.\begin{matrix} U_0{}^c \\ V_0{}^c \end{matrix}\right\} = 2\pi j \operatorname*{res}_{\nu = 1/2} [\text{integrands in (6a) and (6b)}]$$

$$= -jP_0{}^{-1}(-\cos\theta) \begin{cases} j_0(kr)/j_0'(ka), & (7a) \\ j_0'(kr)/j_0(ka). & (7b) \end{cases}$$

In (6a) and (6b), c_ν is the integration contour enclosing the poles $\nu = n + 1/2$ ($n = 0, 1, 2, \cdots$) as shown in Fig. 2. Since c_ν can be distorted into the integration paths l_1, l, and l_2 and the contributions of the integrands in (6a) and (6b) vanish along the integration paths l_1 and l_2, we obtain the following equations:

$$\left.\begin{matrix} U^c \\ V^c \end{matrix}\right\} = \int_l [\text{integrands in (6a) and (6b)}]\, d\nu.$$

U^c and V^c given by (6) are similar to those appearing in the problem of the vertical electric source and the method described in [8] is available to obtain the expressions for the open spherical surface. By eliminating the terms which are odd functions with respect to ν and employing the method of Babich and Buldyrev [5], U^o and V^o corresponding to the expressions for the open spherical surface can be expressed as follows:

$$\left.\begin{matrix} U^o \\ V^o \end{matrix}\right\} = \mp\frac{j}{2}\int_l d\nu\nu E_1{}^{(2)}(\nu,\theta) \cdot \begin{cases} \dfrac{W_p(r,a)}{h_p{}^{(1)\prime}(ka) j_p'(ka)}\, d\nu, & (8a) \\ \dfrac{W_p(a,r)}{h_p{}^{(1)}(ka) j_p(ka)}\, d\nu, & (8b) \end{cases}$$

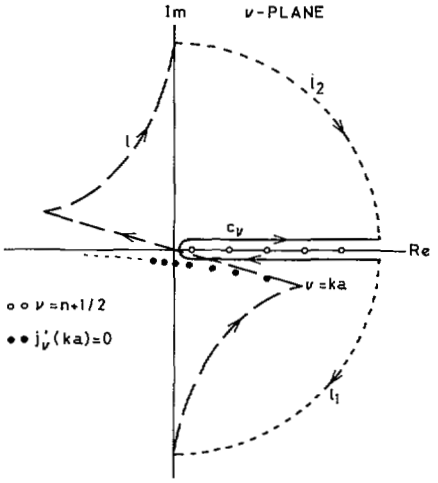

Fig. 2. Integration path c_ν and its deformation in complex ν plane.

where

$$W_p(r,a) = h_p{}^{(2)}(kr)h_p{}^{(1)\prime}(ka) - h_p{}^{(1)}(kr)h_p{}^{(2)\prime}(ka). \tag{9}$$

The function $E_1{}^{(2)}$ denotes the "traveling wave" Legendre function [10],

$$E_1{}^{(2)}(\nu,\theta) = \frac{j}{\sin p\pi}[P_p{}^{-1}(-\cos\theta) - e^{-j(p-1)\pi}P_p{}^{-1}(\cos\theta)] \tag{10}$$

$$\sim \frac{j}{\nu}\sqrt{\frac{2}{\nu\pi\sin\theta}}\, e^{-j(\nu\theta-\pi/4)}, \qquad (|\nu|\to\infty). \tag{11}$$

The functions U^o and V^o given by (8a) and (8b) describe waves reaching the observation point along a direct propagation path and not having periodic properties with respect to θ.

The functions $U_0{}^c$ and $V_0{}^c$ given by (7a) and (7b) are standing wave type functions with respect to r and θ, and they are inadequate as expressions for the fields related to the open spherical surface. In order to obtain traveling wave expressions with respect to r, the following expansion has been introduced by assuming a small negative imaginary part of the propagation constant k:

$$j_0(kr)/j_0'(ka) \sim -je^{jk(r-a)}\sum_{n=0}^{\infty}(-e^{-j2ka})^n + je^{-jk(r+a)}\sum_{m=0}^{\infty}(-e^{-j2ka})^m. \tag{12}$$

A similar expansion is also introduced for $j_0'(kr)/j_0(ka)$. The term for $n = 0$ in (12) expresses the traveling wave generated by the source on the surface and the term for $m = 0$ is interpreted as a reflected wave emanating from the origin. The remaining terms for $n = 1, 2, 3, \cdots$ and $m = 1, 2, 3, \cdots$ correspond to repeatedly reflected waves. If such an interpretation is valid, we can take the zeroth order term ($n = 0$) as the expression for the case of an open spherical surface. With this

procedure, U_0^o and V_0^o can be obtained as follows:

$$\left.\begin{matrix} U_0^o \\ V_0^o \end{matrix}\right\} = \mp P_0^{-1}(-\cos\theta)e^{jk(r-a)}$$

$$= \pm \cot\frac{\theta}{2} e^{jk(r-a)}, \tag{13}$$

which gives

$$\frac{\partial}{\partial\theta} U_0^o - \frac{V_0^o}{\sin\theta} = 0, \qquad \frac{U_0^o}{\sin\theta} - \frac{\partial}{\partial\theta} V_0^o = 0. \tag{14}$$

Equation (14) means that there is no contribution from U_0^o and V_0^o to the fields at an open spherical surface.

Thus the magnetic fields inside the open spherical surface are formulated as follows.

$$\left.\begin{matrix} H_\theta \\ H_\phi \end{matrix}\right\} = \mp \frac{M_0}{4\pi\zeta_0 ar}$$

$$\left\{\begin{matrix} \cos\phi \left[\dfrac{U^o(r,\theta)}{\sin\theta} - \dfrac{\partial}{\partial\theta} V^o(r,\theta)\right] & (15a) \\ \sin\phi \left[\dfrac{\partial}{\partial\theta} U^o(r,\theta) - \dfrac{V^o(r,\theta)}{\sin\theta}\right]. & (15b) \end{matrix}\right.$$

The validity of (15a) and (15b) will be discussed in the following sections.

III. HIGH-FREQUENCY SURFACE FIELDS

In this section, interest is focused on the surface fields. By setting the observation point on the boundary ($r = a$), the functions U^o and V^o are expressed as

$$\left.\begin{matrix} U^o(\theta) \\ V^o(\theta) \end{matrix}\right\} = \pm \int_l \nu E_1^{(2)}(\nu,\theta)$$

$$\cdot \left\{\begin{matrix} 1/[h_p'^{(1)}(ka) j_p'(ka)]\, d\nu & (16a) \\ 1/[h_p^{(1)}(ka) j_p(ka)]\, d\nu. & (16b) \end{matrix}\right.$$

Some asymptotic representations can be obtained from (16a) and (16b) under the condition that the radius of the spherical surface is much greater than the wavelength. Ishihara *et al.* [4], [7] have compared some numerical results of the surface field obtained by using the following asymptotic representations for the case of cylindrical concave surface: a) ray plus canonical integral representation; b) whispering gallery (WG) mode sum and continuous spectrum representation; c) ray plus WG mode representation; and d) near-field representation. First derivation of b) and c) appeared in [3], and a) was derived in [5]. Similar methods are also applicable to (16a) and (16b) to obtain high-frequency field representations. We observe that the WG mode and continuous spectrum representation is not convenient to compute the fields on the concave spherical surface. The reason is that the calculation of the Legendre function $P_p^{-1}(-\cos\theta)$ in (10) and evaluation of the WG mode are difficult when θ is very small and ν is not a large number. Therefore, we have adopted the method of representing the fields in terms of rays and simplified integrals.

The procedure for deriving the high-frequency representations is similar to those in the case of a vertical electric source on a spherical surface [8].

By utilizing partial expansions for $1/j_p'$ and $1/j_p$ in (16a) and (16b),

$$\frac{1}{j_p'(ka)} = \frac{2}{h_p'^{(1)}(ka)} \sum_{n=0}^{N} [-q]^n + \frac{1}{j_p'(ka)} [-q]^{N+1},$$

$$q = \frac{h_p'^{(2)}(ka)}{h_p'^{(1)}(ka)}, \tag{17}$$

the functions U^o and V^o can be divided into two parts:

$$\left.\begin{matrix} U^o \\ V^o \end{matrix}\right\} = \sum_{n=0}^{N} \left\{\begin{matrix} U_n^g \\ V_n^g \end{matrix}\right\} + \left\{\begin{matrix} U_N^R, & (18a) \\ V_N^R, & (18b) \end{matrix}\right.$$

where U_n^g and V_n^g correspond to the nth terms of the partial expansions and U_N^R, V_N^R correspond to the remaining terms. The spherical Bessel functions $h_p^{(1,2)}$ and the traveling Legendre function $E_1^{(2)}$ involved in the expressions of U_n^g and V_n^g are replaced, respectively, by the Debye asymptotic forms [4] and (11). By deforming the integration path into the steepest descent path in the w plane ($w = \arcsin(\nu/ka)$), one can express the functions U_n^g and V_n^g as ray optical representations. The remaining integrals U_N^R and V_N^R can be simplified with the aid of the Fock asymptotic approximations of the Bessel functions [4], [11]. Changing the variables to t via $\nu = ka + (ka/2)^{1/3}t$ and taking into account that the principal contribution to the integrals arises at the vicinity of $t = 0 (\nu = ka)$ [4], one can express the functions U_N^R and V_N^R in terms of simplified integrals. Equation (11) is again used in the above transformations.

Substituting the simplified forms of U_n^g, V_n^g, U_N^R and V_N^R into (15a) and (15b), one can obtain the asymptotic expressions of the surface magnetic fields excited by the horizontal magnetic source as follows:

$$H_\theta(\theta,\phi) \sim \sum_{n=0}^{N} H_{\theta n}^g(\theta,\phi) + H_{\theta N}^R(\theta,\phi), \tag{19a}$$

$$H_\phi(\theta,\phi) \sim \sum_{n=0}^{N} H_{\phi n}^g(\theta,\phi) + H_{\phi N}^R(\theta,\phi), \tag{19b}$$

where $H_{\theta n}^g$ and $H_{\phi n}^g$ account for the contribution of U_n^g, V_n^g and are given by

$$\left.\begin{matrix} H_{\theta n}^g \\ H_{\phi n}^g \end{matrix}\right\} = j\frac{kM_0}{\pi\zeta_0} \left[\cos\frac{\theta}{2(n+1)}\right]^{1/2} \frac{e^{-jkr_n}}{\sqrt{ar_n \sin\theta}}$$

$$\left\{\begin{matrix} (-j)^n \cos\phi \sin^2\dfrac{\theta}{2(n+1)}, & (20a) \\ j^n \sin\phi, & (20b) \end{matrix}\right.$$

$$r_n = 2a(n+1)\sin\frac{\theta}{2(n+1)}. \tag{20c}$$

In the above equations, $H_{\theta n}^g$ and $H_{\phi n}^g$ describe the geometrical optics fields having been reflected n times and r_n denotes

their ray paths. For $n = 0$, they are four times as large as the magnetic fields radiated from a magnetic point source in free space, and for n greater than unity, they are identical to the fields obtained by using geometrical optics [12]. This indicates that (15a) and (15b) are valid expressions of the fields inside the open spherical concave surface.

The remaining terms $H_{\theta N}{}^{R}$ and $H_{\phi N}{}^{R}$ account for the contribution of $U_N{}^{R}$ and $V_N{}^{R}$ and are given by

$$\left.\begin{matrix} H_{\theta N}{}^{R} \\ H_{\phi N}{}^{R} \end{matrix}\right\} = \mp jM_0 \frac{e^{-j(kS-\pi/4)}}{4\pi^{5/2}\zeta_0 a^2\sqrt{\sin\theta}} \left\{ \begin{matrix} \cos\phi \left[\xi \frac{I_N(\gamma)}{\sin\theta} + \xi^{-1} J_N{}'(\gamma) \right. \\ \left. - \xi^{-3}\left(\frac{\cot\theta}{2} + jka\right) J_N(\gamma) \right] \end{matrix} \right. \tag{21a}$$

$$\left. \begin{matrix} \sin\phi \left[\xi^{-3} \frac{J_N(\gamma)}{\sin\theta} + \xi^{3} I_N{}'(\gamma) \right. \\ \left. - \xi\left(\frac{\cot\theta}{2} + jka\right) I_N(\gamma) \right], \end{matrix} \right. \tag{21b}$$

$$\xi = (ka/2)^{1/6}, \qquad \gamma = (ka/2)^{1/3} S/a, \qquad S = a\theta, \tag{21c}$$

where

$$I_N(\gamma) = \int_{l_t} \frac{e^{-j\gamma t}}{w_1{}'(t) A_i{}'(t)} \left[-\frac{w_2{}'(t)}{w_1{}'(t)} \right]^{N+1} dt, \tag{22a}$$

$$J_N(\gamma) = \int_{l_t} \frac{e^{-j\gamma t}}{w_1(t) A_i(t)} \left[-\frac{w_2(t)}{w_1(t)} \right]^{N+1} dt, \tag{22b}$$

$$\left.\begin{matrix} I_N{}'(\gamma) \\ J_N{}'(\gamma) \end{matrix}\right\} = \frac{d}{d\gamma} \left\{ \begin{matrix} I_N(\gamma), & (22c) \\ J_N(\gamma), & (22d) \end{matrix} \right.$$

$$w_{1,2}(t) = A_i(t) \mp jB_i(t), \tag{22e}$$

and A_i, B_i denote the Airy functions. The integration contour l_t in the complex t plane is illustrated in Fig. 3. $H_{\theta N}{}^{R}$ and $H_{\phi N}{}^{R}$ given by (21a) and (21b) describe the effects of ray fields having been reflected more than N times and involve the simplified integrals I_N, J_N, $I_N{}'$, and $J_N{}'$. The integral I_N is the same as that in the case of a cylindrical surface [4] except for the sign $(-1)^{N+1}$. These integrals can be computed efficiently by deforming the integration path l_t into $t = \infty e^{-j\pi/3} \to \infty e^{j2\pi/3}$ [5] as shown in Fig. 3.

The number of rays $N + 1$ is determined such that, when the arc length parameter γ is increased, $N + 1$ also increases. In the region near the source, no ray-optical contribution is included, i.e., $N = -1$. The criterion for choosing the number of rays has been discussed in [3]-[5].

As the limiting case of $\gamma \to 0$ in (22a) and (22b), we obtain the following near-field representations:

$$I_{-1}(\gamma) \sim \frac{2\pi^{3/2}}{\sqrt{\gamma}} e^{j\pi/4} \sum_{n=0}^{\infty} b_n \gamma^{3n/2}, \tag{23a}$$

$$J_{-1}(\gamma) \sim \frac{2\pi^{3/2}}{\gamma^{3/2}} e^{-j\pi/4} \sum_{n=0}^{\infty} d_n \gamma^{3n/2}, \tag{23b}$$

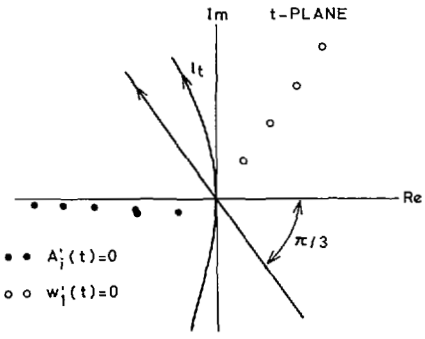

Fig. 3. Integration paths in complex t plane.

where b_n is the coefficient found in [4] (note that $-i$ in [4] should be replaced by j in this case) and d_n is given by

$$d_0 = -1/2,\ d_1 = 0.25\sqrt{\pi}e^{-j3\pi/4},\ d_2 = -j0.2083,$$
$$d_3 = 0.390625 \times 10^{-1}\sqrt{\pi}e^{-j\pi/4},\ d_4 = 0.1827042 \times 10^{-1}$$
$$d_5 = -0.2298983 \times 10^{-2}\sqrt{\pi}e^{-j3\pi/4},$$
$$d_6 = j0.7978640 \times 10^{-3},$$
$$d_7 = -0.3971226 \times 10^{-4}\sqrt{\pi}e^{-j\pi/4},$$
$$d_8 = -0.2116366 \times 10^{-4},$$
$$d_9 = 0.1933803 \times 10^{-5}\sqrt{\pi}e^{-j3\pi/4},$$
$$d_{10} = -j0.4814811 \times 10^{-6}. \tag{24}$$

Equations (23a) and (23b) are valid either when the observation point approaches the source point or when the radius of the spherical surface becomes infinite. In fact, substituting (23a) and (23b) into (21a) and (21b) and letting $\gamma \to 0$, one obtains

$$\left.\begin{matrix} H_\theta \\ H_\phi \end{matrix}\right\} \sim -jM_0 \frac{e^{-jkS}}{2\pi\zeta_0} \left\{ \begin{matrix} \cos\phi \left[j\frac{2}{S^2} + \frac{2}{kS^3} \right], & (25a) \\ \sin\phi \left[\frac{1}{kS^3} + j\frac{1}{S^2} - \frac{k}{S} \right], & (25b) \end{matrix} \right.$$

which are exactly the same as the fields excited by a horizontal magnetic point source located on an infinitely large conducting plane. This observation is considered to be another corroboration of the validity of (15a) and (15b).

IV. THEORETICAL AND EXPERIMENTAL RESULTS

The surface magnetic fields excited by a horizontal magnetic point source located on a conducting concave spherical surface can be calculated by using (19a)-(24). Numerical calculation has been performed by varying the values of N. These curves for various N are superposed for a wide range of the arc distance S in a similar fashion as in the case of the vertical electric source on a concave spherical surface [8] and magnetic sources on a concave cylindrical surface [4], [6], [7]. Fig. 4 shows the amplitude of the surface field H_ϕ as a function of the arc distance S with $ka = 104.7$ and $\phi = 90°$.

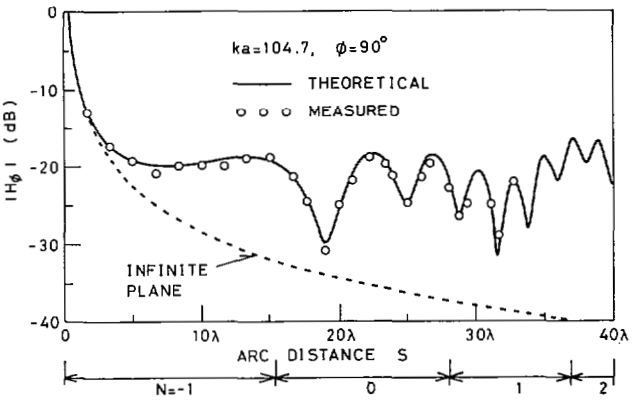

Fig. 4. Amplitude of normalized surface field H_ϕ. Theoretical values and measured data are both normalized to 0 dB at $S/\lambda = 1/3$.

In order to confirm the validity of the theoretical results, experimental investigation has been performed. The frequency used is 10.0 GHz, and the radius of the conducting hemisphere is 0.5 m ($ka = 104.7$) [8]. The surface magnetic field excited by a small slot antenna was measured by a pickup shielded loop antenna. The length of the slot antenna is about $\lambda/4$, and it was fed by a standard X-band waveguide. The radius of the loop antenna is about $\lambda/24$, and its output was delivered to a spectrum analyzer through a semirigid cable (radius is about $\lambda/75$) creeping over the concave surface. Diffraction at an edge of the hemisphere was avoided with absorbing material located around the edge.

The measured amplitude of the surface magnetic field H_ϕ is shown in Fig. 4 and compared with the theoretical results. Theoretical values and measured data are both normalized as 0 dB at the point where $S = 1$ cm ($S/\lambda = 1/3$). The agreement between the theory and the measurements is fairly good, and the validity of the analysis described in Sections II and III is confirmed.

V. MUTUAL COUPLING BETWEEN SLOTS

By employing the results described in Section III, the mutual coupling between slot antennas located on a concave spherical surface can be estimated. The stationary expression for the self- and mutual admittance of slot antennas excited by rectangular waveguides is given by

$$Y_{ij} = \iint_{S_i} (\mathbf{E}_i \times \mathbf{H}_j) \cdot d\mathbf{S}/(V_i V_j), \tag{26}$$

where $\mathbf{E}_i$ denotes the surface electric field produced when the dominant mode voltage V_i is applied to the ith aperture with all other apertures shorted. The surface magnetic field $\mathbf{H}_j$ is similarly produced when V_j is applied to jth aperture with all other apertures shorted.

Since the dominant mode in the rectangular waveguide is the TE_{10} mode, the electric field $\mathbf{E}_i$ may be assumed to be that of TE_{10} mode in the sense of a first-order approximation. The surface field $\mathbf{H}_j$ can be obtained from

$$\mathbf{H}_j(\mathbf{r}) = \iint_{S_j} \bar{\bar{G}}(\mathbf{r}, \mathbf{r}') \cdot \mathbf{n} \times \mathbf{E}_j(\mathbf{r}')\, dS', \tag{27}$$

where $\bar{\bar{G}}(\mathbf{r}, \mathbf{r}')$ is the dyadic Green's function which describes

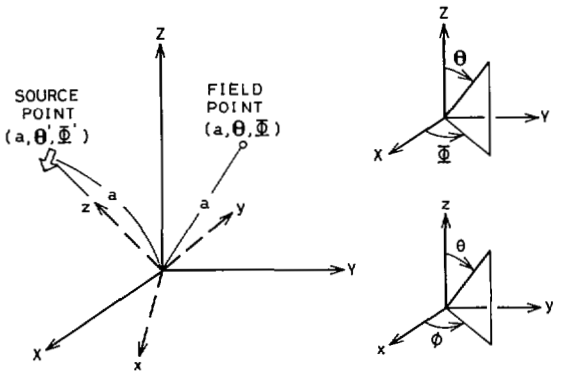

Fig. 5. Coordinate systems for calculating mutual coupling.

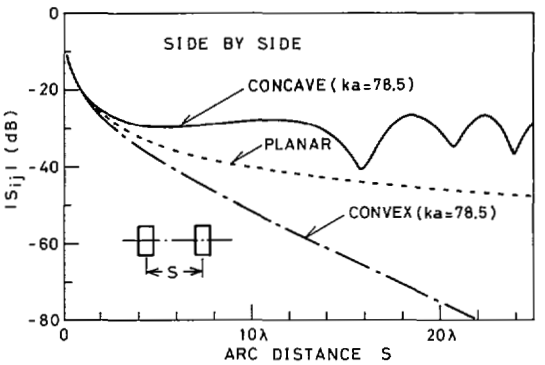

Fig. 6. Amplitude of S_{ij} for side-by-side slot antennas on concave, convex, and planar surfaces.

the surface magnetic fields of a magnetic point source located at $\mathbf{r} = \mathbf{r}'$. In (27), the source point and direction are arbitrary. In order to have the source always located on the z-axis and directed parallel to the x-axis, it is convenient to introduce a local coordinate system xyz as shown in Fig. 5. The relations between the coordinate systems xyz and XYZ are found in [9] and [13]. By using the coordinate transformation and (19a)–(24), the mutual admittance has been computed numerically.

The coupling coefficient S_{ij} is given by

$$S_{ij} = \frac{-2Y_g Y_{ij}}{(Y_g + Y_{ii} + Y_{ij})(Y_g + Y_{ii} - Y_{jj})} \tag{28}$$

where Y_{ii} and Y_g denote the self-admittance and characteristic admittance for TE_{10} mode, respectively. When the radius of the spherical surface a is much greater than the wavelength λ, the self-admittance Y_{ii} can be assumed to be that of a slot antenna in an infinite conducting plane.

Figs. 6–8 show the computed results of the amplitude of S_{ij} for the case of side-by-side, in echelon, and collinear slot antennas. For comparison, the mutual coupling between slot antennas on an infinite conducting plane and a conducting convex spherical surface obtained by Nakashima *et al.* [9] is also plotted in Figs. 6–8. The dimensions of the slot antenna are $0.797\lambda \times 0.397\lambda$ and the radius of the spherical surface is $a = 12.5\lambda$ ($ka = 78.5$).

On the convex side, $|S_{ij}|$ decays rapidly as the arc distance S is increased. On the other hand, it does not decay and shows oscillatory behavior on the concave side. This tendency can be deduced from the results shown in Fig. 4, which illustrates the surface magnetic field excited by a magnetic point source.

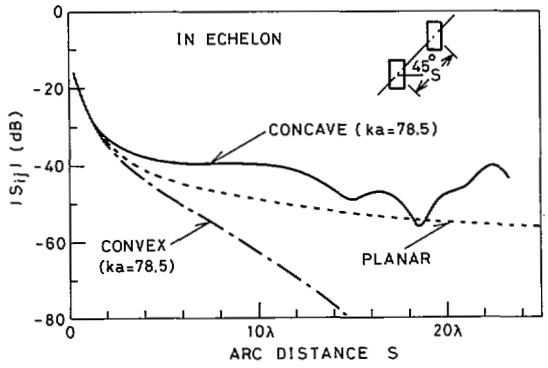

Fig. 7. Amplitude of S_{ij} for slot antennas in echelon.

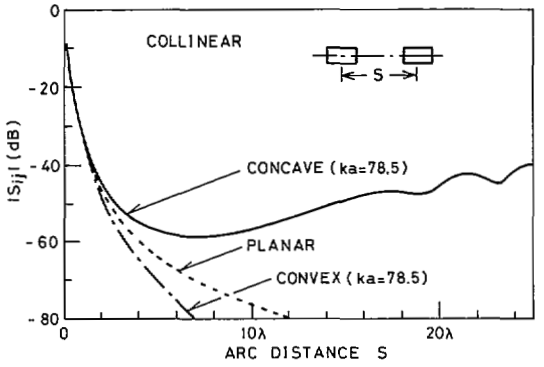

Fig. 8. Amplitude of S_{ij} for collinear slot antennas.

VI. MEASUREMENT OF THE MUTUAL COUPLING

In order to compare with the theoretical results described in the previous sections, experiments have been performed. The apertures of slot antennas were excited with rectangular waveguides and have the same cross sectional dimensions as the feed waveguide. Dimensions of apertures and radius of a conducting hemisphere are the same as those in Figs. 6–8. The frequency used here is 50 GHz.

The measured amplitude of mutual coupling coefficient between side-by-side slot antennas on a concave surface is illustrated in Fig. 9 and compared with the theoretical values. The measured values agree qualitatively with the theoretical ones but are somewhat less than the theoretical values. These disagreements can be partly attributed to the effect of higher order modes which appear in the apertures of slot antennas. Recent investigation of the mutual coupling coefficient between rectangular slot antennas on a conducting planar surface [14] shows that the effect of higher order modes is not serious, but it introduces a slight reduction for the amplitude of the mutual coupling coefficient. The remaining part of the deviation has not been explained as yet.

VII. CONCLUSION

The expressions of the surface fields excited by a horizontal magnetic point source located on a conducting concave spherical surface have been derived. Although the method employed in this analysis is similar to that for the case of a cylindrical surface, the present investigation is the first attempt with sources on an open spherical surface. The analysis

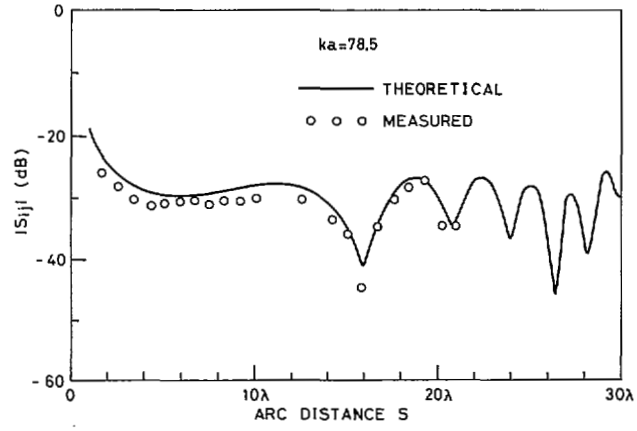

Fig. 9. Comparison between theoretical and measured data of amplitude of S_{ij} between side-by-side slot antennas on concave surface.

has been extended to the mutual coupling between slot antennas on the concave side. The calculated results for the surface fields agree with experimental data.

The mutual coupling between slot antennas on the concave surface has been calculated by assuming the dominant mode field of a rectangular waveguide in the aperture. Numerical results are compared with those for the cases of planar and convex surfaces. On the concave side, the amplitude of the mutual coupling does not decay and shows oscillatory behavior when the arc distance is increased. On the other hand, it decays rapidly on the convex side. These theoretical results for the mutual coupling in the case of concave side have been confirmed by the experiment showing the validity of the analysis presented in this paper.

ACKNOWLEDGMENT

The authors express their thanks to Dr. Takayuki Ishizone, Mr. Yutaka Nakashima, and Mr. Hironobu Tachimura for their helpful discussions.

REFERENCES

[1] L. Schwartzman and J. Stangel, "The dome antenna," *Microwave J.*, vol. 18, pp. 31–34, Oct. 1975.
[2] H. Steyskal, A. Hessel, and J. Shmoys, "On the gain-versus-scan trade-offs and the phase gradient synthesis for a cylindrical dome antenna," *IEEE Trans. Antennas Propagat.*, vol. AP-27, pp. 825–831, Nov. 1979.
[3] W. Wasylkiwskyj, "Diffraction by a cncave perfectly conducting circular cylinder," *IEEE Trans. Antennas Propagat.*, vol. AP-23, pp. 480–492, Jul. 1975.
[4] T. Ishihara, L. B. Felsen, and A. Green, "High-frequency fields excited by a line source located on a perfectly conducting concave cylindrical surface," *IEEE Trans. Antennas Propagat.*, vol. AP-26, pp. 757–767, Nov. 1978.
[5] V. M. Babich and V. S. Buldryrev, *Asymptotic Methods of Short* Wave Diffraction. Moscow, USSR; Nauka, 1972, ch. 11.
[6] T. Ishihara and L. B. Felsen, "High-frequency fields excited by a line source located on a concave cylindrical impedance surface," *IEEE Trans. Antennas Propagat.*, vol. AP-27, pp. 172–179, Mar. 1979.
[7] L. B. Felsen and T. Ishihara, "High-frequency surface fields excited by a point source on a concave perfectly conducting cylindrical boundary," *Radio Sci.*, vol. 14, pp. 205–216, Mar.–Apr. 1979.

[8] K. Inami, K. Sawaya, and Y. Mushiake, "Surface fields excited by a vertical electric point source located on a conducting concave spherical surface," *Trans. IECE Japan*, vol. J64-B, pp. 1008–1015, Sept. 1981.
[9] Y. Nakashima, K. Sawaya, T. Ishizone, and Y. Mushiake, "The mutual admittance of slots on the sphere," IECE Japan, Tech. Rep. AP79-53, Aug. 1979.
[10] L. B. Felsen and N. Marcuvitz, *Radiation and Scattering of Waves*. Englewood Cliffs, NJ: Prentice-Hall, 1973.
[11] M. Abramowitz and I. A. Stegun, *Handbook of Mathematical Functions*. New York: Dover, 1970, ch. 10.
[12] R. G. Kouyoumjian and P. H. Pathak, "A uniform geometrical theory of diffraction for an edge in a perfectly conducting surface," *Proc. IEEE*, vol. 62, pp. 1448–1461, Nov. 1974.
[13] S. Horiguchi, "Self and mutual impedance of dipole antennas over a conducting sphere," in *IEEE Student Papers Book*. New York: Oct. 1980.
[14] I. Watanabe, K. Sawaya, T. Ishizone, and Y. Mushiake, "Analysis of mutual coupling coefficient between two rectangular slot antennas taking account of higher order modes in the apertures," in *Proc. Joint Conf. Electr. Eng. Tohoku Branch Japan*, 1981, p. 157.

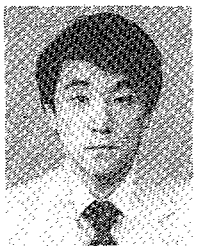

Kazuyoshi Inami was born in Ibaraki-Ken, Japan, on January 15, 1955. he received the B.E. and M.E. degrees from Tohoku University, Sendai, Japan, in 1978 and 1980, respectively.

In 1980 he joined Communication Equipment Works of Mitsubishi Electric Corporation, Amagasaki, Japan. He is now engaged in the development of design of microwave devices.

Mr. Inami is a member of the Institute of Electronics and Communication Engineering of Japan.

Kunio Sawaya (M'79), for a photograph and biography please see page 756 of the September 1981 issue of this TRANSACTIONS.

Yasuto Mushiake (A'55–M'60–F'76), for a photograph and biography please see page 756 of the September 1981 issue of this TRANSACTIONS.

Low Sidelobe Aperture Distributions for Blocked and Unblocked Circular Apertures

ARTHUR C. LUDWIG

Abstract—**Low sidelobe aperture distributions are investigated for both blocked and unblocked circular apertures. Both peak sidelobe levels and wide-angle sidelobe levels are considered. For unblocked apertures, Taylor's circular aperture synthesis technique is generalized to provide control over the wide angle sidelobe decay rate. These distributions are compared to a wide variety of alternative distributions in terms of the beamwidth, aperture efficiency, and radiated power distributions achieved for a given peak sidelobe level. A comparison is also made between the sidelobe envelopes achieved by four different distributions with a fixed beamwidth. For centrally blocked apertures, it is shown that wide angle sidelobes can be reduced by employing aperture distributions with a hole in the blocked central area.**

I. INTRODUCTION

THE SYNTHESIS of low sidelobe antenna patterns is a classic problem with an extensive literature. This paper is intended to contribute in the following three areas:[1]

1) A generalization of Taylor's circular aperture synthesis technique [1] to include control of the wide-angle sidelobe decay rate is presented. The analysis provides results for circular apertures analogous to the results given by Rhodes for line sources [2]. These new distributions provide additional capabilities compared to alternatives such as the Bickmore–Spellmire distributions [3], [4].
2) A unified comparison, for peak sidelobe levels down to 90 dB below the beam peak, of beamwidth, aperture efficiency, and radiated power distributions achieved by a wide variety of circular aperture illuminations is given. These results complement an excellent comparison of linear distributions given by Harris [5].
3) An investigation of methods for reducing wide angle sidelobes introduced by aperture blockage is conducted. Aperture distributions with holes extending over the blocked region are considered. Such distributions raise the first sidelobe, but lower wide-angle lobes.

This paper emphasizes the problem of reducing wide-angle sidelobes. While the peak level criterion will generally be employed, data are also provided on the total power radiated beyond a given angle. This power is easily related to the root mean square (rms) sidelobe level within a given angular sector, and is defined by (1) for a pattern $g(u)$:

$$\Delta P(u_0) \equiv \frac{\int_{u_0}^{\infty} g^2(u) u \, du}{\int_{0}^{\infty} g^2(u) u \, du}. \tag{1}$$

Manuscript received August 11, 1981; revised September 21, 1981. This work was sponsored by the Defense Advanced Research Project Agency under ARPA Order No. 3169, and monitored by MICOM under contract DAAH01-80-C-1056.

The author is with General Research Corporation, P. O. Box 6770, Santa Barbara, CA 93111.

[1] This paper is a condensation of the author's report RM-2367, General Research Corporation, Apr. 1981.

0018-926X/82/0900-0933$00.75